*Journal of Hydraulic Research* Vol. 46, No. 5 (2008), pp. 679–690
doi:10.3826/jhr.2008.2975


# A turbulent approach to unsteady friction

# Une approche turbulente du frottement instationnaire

IVO POTHOF, (IAHR Member), *Specialist Industrial Flow Technology, Deltares|Delft Hydraulics, P.O. Box 177, 2600 MH Delft, The Netherlands. E-mail: Ivo.pothof@deltares.nl; Affiliated with Department of Civil Engineering and Geosciences, Delft University of Technology*

**ABSTRACT**
This paper discusses the existing approaches to unsteady friction and presents some new ideas on the modelling of unsteady friction in turbulent pipe flows. This paper aims to contribute to a physically-based unsteady friction model that captures the known physical characteristics of friction phenomena in transient turbulent pipe flows. For practical applicability, a new model should not require extensive computer memory from previously calculated flows, nor complex iterative procedures, since unsteady friction computations will be carried out in every calculation node at every time step of any transient scenario. A new formulation for the unsteady shear stress is proposed and validated against eight transient scenarios in four different systems, conveying water with steady state Reynolds numbers varying between 1940 and 1.5 million.

**RÉSUMÉ**
Cet article discute des approches existantes pour le frottement instationnaire et présente quelques nouvelles idées sur sa modélisation dans les écoulements turbulents en conduites. Cet article vise à contribuer à un modèle de frottement instationnaire basé sur la physique qui puisse capter les caractéristiques physiques connues des phénomènes de frottement dans des écoulements transitoires turbulents en conduite. Pour une mise en œuvre pratique, un nouveau modèle ne devrait pas exiger la mémoire d'ordinateur étendue des écoulements précédemment calculés, ni des procédures itératives complexes, vu que le frottement instationnaire devra être évalué en chaque nœud de calcul et à chaque pas de temps de tout scénario transitoire. Une nouvelle formulation de l'effort de cisaillement instationnaire est proposée et validée par huit scénarios transitoires dans quatre systèmes différents, transportant l'eau avec des nombres de Reynolds à l'équilibre variant entre 1.940 et 1.5 million.

*Keywords*: Damping, pipe flow, turbulence, unsteady flow, wall friction

## 1 Introduction

The dynamic behaviour of pressure and flow in a pipe system during a transient event (e.g., pump trip, emergency valve closure) is dominated by fluid inertia, fluid compressibility and pipe wall elasticity. These effects cause pressure and flow oscillations which dampen due to internal friction forces and wall friction forces.

The friction forces are traditionally modelled with a constant friction factor or quasi-steady friction factor. It is known that both the constant and quasi-steady friction model underestimate the observed unsteady friction, since measured pressure and velocity signals dampen faster than the calculated pressures.

Unsteady friction modelling has received regular, but no abundant, attention throughout the last century. The reasons for the moderate attention for this subject are logical. For many transient scenarios, the extreme pressures occur during the first wave period, which are reliably predicted by the constant or quasi-steady friction models. A second reason is that unsteady friction modelling is a complex problem. In fact one seeks a turbulence model for transient pipe flows in a one-dimensional (1D) formulation, which can be computed efficiently enough for practical applications. Of course there are plenty of reasons that have motivated researchers during the last century to explore the subject. Apart from scientific interest to solve a complex problem, an unsteady friction model is beneficial for the application of transient-based leak detection methods in transportation pipelines or distribution networks. Unsteady friction is assumed to play an important role in the prediction of sonic booms, caused by high speed trains in long tunnels. Another reason to work on unsteady friction models is the increasing complexity of the operation of pipe systems. The anti-surge provisions become more and more integrated with the operational control system, which in turn gets more automated by SCADA system applications. The effect of this integration on the hydraulic design of new pipe systems or on the de-bottlenecking of existing systems is that transient simulations tend to cover larger time horizons including multiple transient events. An example of such a transient scenario is a

Revision received March 10, 2008/Open for discussion until April 30, 2009.

pump trip and automatic restart of the pumping station by a back-up power supply. If the restart is preferably carried out as soon as possible—e.g., to prevent loss of cooling capacity or production quality—then the correct prediction of the damping of the initial surge pressures may significantly affect the earliest restart time.

This paper discusses the existing approaches to unsteady friction and presents some new ideas on the modelling of unsteady friction in turbulent pipe flows. The paper aims to contribute to an unsteady friction model that captures the known physical characteristics of friction phenomena in transient turbulent pipe flows. It will be kept in mind that any new model should not require extensive computer memory to store previously calculated flows, nor complex iterative procedures, because the unsteady friction computations have to be carried out in every calculation point and at every time step of a transient scenario with an extensive time horizon.

A new formulation for the unsteady shear stress is proposed and validated against eight transient scenarios in four different systems, conveying water with steady state Reynolds numbers varying between 1940 and 1.5 million.

Throughout this paper the following convention on decelerating and accelerating flows applies in order to prevent unnecessarily complex sentences: the flow is called decelerating if the absolute velocity reduces and accelerating if the absolute velocity increases.

## 2 Existing unsteady friction models

An excellent review paper on water hammer theory, including extensive discussions of the existing unsteady friction models, has been written by Ghidaoui *et al.* (2005). Ghidaoui *et al.* distinguish empirical-based and physically-based unsteady friction approaches. Both approaches model the unsteady wall shear stress as a correction to the steady or quasi-steady wall shear stress:

$$\tau_{tot} = \tau_s + \tau_{uf} \tag{1}$$

or

$$\tau_{tot} = \tau_{qs} + \tau_{uf} \tag{2}$$

The subscript $s$ refers to the steady state preceding the transient event, while the subscript $qs$ refers to the quasi-steady state derived from the instantaneous velocity. The following relation between the total, (quasi)-steady and unsteady friction factor is a direct consequence of Eqs (1) and (2):

$$f_{tot} = f_s + f_{uf} \tag{3}$$

or

$$f_{tot} = f_{qs} + f_{uf} \tag{4}$$

It must be noted that the difference in transient results between the constant steady friction factor and the quasi-steady friction factor is marginal for valve closure scenarios.

The most widely known empirical-based (or instantaneous acceleration) unsteady friction models have been proposed by Daily *et al.* (1956) and Brunone (1991). Brunone's model has been refined by Pezzinga (2000) and Bergant *et al.* (2001). Daily's *et al.* (1956) and Bergant's *et al.* (2001) wall shear stress formulations are as follows:

$$\tau_{uf} = k \cdot \frac{\rho D}{4} \frac{\partial v}{\partial t} \tag{5}$$

$$\tau_{uf} = k \cdot \frac{\rho D}{4} \left[ \frac{\partial v}{\partial t} + c \cdot \mathrm{sgn}(v) \left| \frac{\partial v}{\partial x} \right| \right] \tag{6}$$

Vítkovský *et al.* (2006) have shown that the empirical-based unsteady friction has shown deficient for certain generic types of transient events.

The most widely known physically-based unsteady friction models have been proposed by Zielke (1968) and Vardy and Brown (1993, 1995, 2003, 2004). Zielke's unsteady friction model is based on the analytical solution of unsteady laminar pipe flow, which leads to a convolution integral over the past decelerations. Vardy and Brown extended Zielke's formulation to turbulent pipe flows by making an assumption on the shear stress distribution and by assuming the turbulent eddy viscosity to be time-invariant (i.e. frozen to its steady state value). Vardy's frozen viscosity is assumed to be linearly increasing in a wall annulus and constant in the core region as detailed in Vardy and Brown (2003) for smooth pipe walls and in Vardy and Brown (2004) for rough walls. Vardy's refined model of the wall shear stress for smooth walled pipes, Vardy and Brown (2003), is as follows:

$$\tau_{uf} = \frac{4\rho\nu}{D} \int_{\theta}^{\mathrm{T}} W(T-\theta) \frac{\partial v}{\partial t} \, d\theta$$
$$W(\theta) = \frac{1}{2\sqrt{\pi\psi}} \exp(-\psi/C^*) \tag{7}$$

and

$$\psi = \frac{\nu_{lam}\theta}{R^2}$$
$$C^* = \frac{12.86}{\mathrm{Re}^{\kappa}}; \quad \kappa = \log_{10}\left(\frac{15.29}{\mathrm{Re}^{0.0567}}\right) \tag{8}$$

where the Reynolds numbers in Eq. (8) apply to the steady state values preceding the transient event. Vítkovský *et al.* (2006) conclude that the physically-based unsteady friction models correctly simulate all transient event types. This conclusion was based on a comparison with low Reynolds number experiments in the Adelaide system; see Sec. 5. Vardy and Brown (2007) have recently extended their weighting function approach to cover the whole range of turbulent flows from fully smooth to fully rough over a wide range of Reynolds numbers.

## 3 Discussion of existing models

Carsten and Roller (1959) have shown that Daily's model (5) can be derived by assuming that the unsteady velocity profiles obey a power law velocity profile. During any flow deceleration a vortex sheet develops and flow reversal occurs close to the pipe wall. This observation limits the applicability of Daily's model to accelerating flows.

Vardy's model (7) reduces to Daily's model (5), if the acceleration is constant. Vardy's analysis (1959) couples the history shear stress models with the instantaneous shear stress models. If the accelerations remain more or less constant for at least a certain limiting time, then this history shear stress model is reasonably approximated by an instantaneous shear stress model. The following expression for the limiting time has been derived by Vardy and Brown (2003):

$$t_{lim} = 3.323 \cdot C^* \tag{9}$$

where $C^*$ has been defined in Eq. (8).

An evaluation of the limiting time for typical pipe sizes and velocities shows that the limiting time is of the order of magnitude of 1 ms. Vardy concludes that if the simulation time step far exceeds the limiting time, then the physically-based history shear stress model and the empirical-based instantaneous shear stress model should yield similar predictions Vardy *et al.* (1993), Vardy and Brown (2003). Consequently in many practical applications with a simulation timestep in the range of 0.1 s to 1 s both models will yield similar predictions.

Three aspects of the existing unsteady shear stress models are discussed below:

- Validity of initial Reynolds number influence;
- Linearity in $dv/dt$;
- Symmetry.

### *3.1 Validity of initial Reynolds number influence*

One drawback of the existing models is the importance of the initial Reynolds number. Excellent measurements on accelerating and decelerating pipe flows, carried out by He and Jackson (2000), confirm that the turbulent viscosity on the centreline remains frozen only during the turbulence diffusion time, defined by:

$$T_d = \frac{D}{u_* \sqrt{2}} \tag{10}$$

where the constant $\sqrt{2}$ has been experimentally confirmed.

Ghidaoui *et al.* (2002) have proposed a logical dimensionless parameter as the ratio of the turbulence diffusion time scale to the waterhammer time scale:

$$P = \frac{T_d}{L/c} = \frac{c \cdot D}{L \cdot u_* \sqrt{2}} = \frac{c \cdot D \sqrt{8}}{L \cdot v_s \sqrt{f2}} = \frac{2c \cdot D}{L \cdot v_s \sqrt{f}} = \frac{2}{\sqrt{f}} \frac{D}{L} \frac{1}{M} \tag{11}$$

The relevance of this dimensionless parameter is best explained with the reservoir—pipe—valve system. If a steep pressure wave passes the midpoint of the pipeline, then the average velocity remains more or less constant for a period $L/c$; i.e., the time the pressure wave needs to travel to a boundary and back to the middle of the pipeline. If $P$ is small ($P \ll 1$), then the turbulence structure has the time to completely adapt to this new pipeline velocity, before the next pressure wave distorts the velocity profile. If $P$ is large ($P \gg 1$), then the velocity profile has not adjusted at all after a pressure wave passage and all velocity disturbances only affect the turbulence intensity in a small layer close to the pipe wall. Ghidaoui *et al.* claim that the quasi-steady assumption is acceptable for $P \gg 1$, which is correct for the turbulence structure in the core of the pipeline, but highly questionable for the turbulence structure close to the wall.

Many typical pipeline systems have a $L/D$ ratio in the order of $10^4$, a Mach number of $10^{-3}$ and an initial friction factor of 0.02, resulting in a typical turbulence diffusion-waterhammer time scale ratio of 1.4. Unfortunately, we have to conclude that many real-life pipeline systems and laboratory systems have a diffusion-waterhammer time scale ratio of order 1 ($0.1 < P < 10$), implying that the turbulence structure is completely mixed by subsequent pressure waves and that the quasi-steady assumption is certainly not applicable. In fact, these typical systems would need a transient turbulence model to predict the dynamic behaviour of the turbulence structure and the consequential transient pressures and flows. The fact that 1D transient turbulence models are not yet available motivates the development of empirical-based unsteady friction models. Another consequence of the turbulence diffusion-waterhammer time scale ratio of order 1 is that the initial turbulence structure is completely renewed every pipe period. Hence the influence of the initial Reynolds number must have vanished after one pipe period already. This paper proposes a new model that explicitly takes the turbulence diffusion time scale into account, such that the initial Reynolds number influence has vanished after the turbulence diffusion time scale.

### *3.2 Linearity in dv/dt*

All transient shear stress models include a common assumption that the transient shear stress is linear in the acceleration. Although this relation has been analytically derived for laminar transient flows, there is no physical mechanism that supports this assumption for turbulent transient flows.

### *3.3 Symmetry*

The main drawback of the existing transient shear stress models however, is the presumed symmetry in the shear stress equation. Both the instantaneous and history shear stress models implicitly assume that the unsteady shear stress is symmetric in the acceleration, i.e.:

$$\tau_{uf}\left(\frac{dv}{dt}\right) = -\tau_{uf}\left(-\frac{dv}{dt}\right) \tag{12}$$

This assumption neglects the physical observations that the unsteady shear stresses are caused by different phenomena during acceleration and deceleration. During flow decelerations a vortex sheet develops in a wall annulus, as depicted in Fig. 1. During flow accelerations these vortices are absent and unsteady friction may only develop due to increased velocity gradients near the pipe wall. These observations support unsteady friction models, that explicitly account for the physical differences between accelerating and decelerating flows.

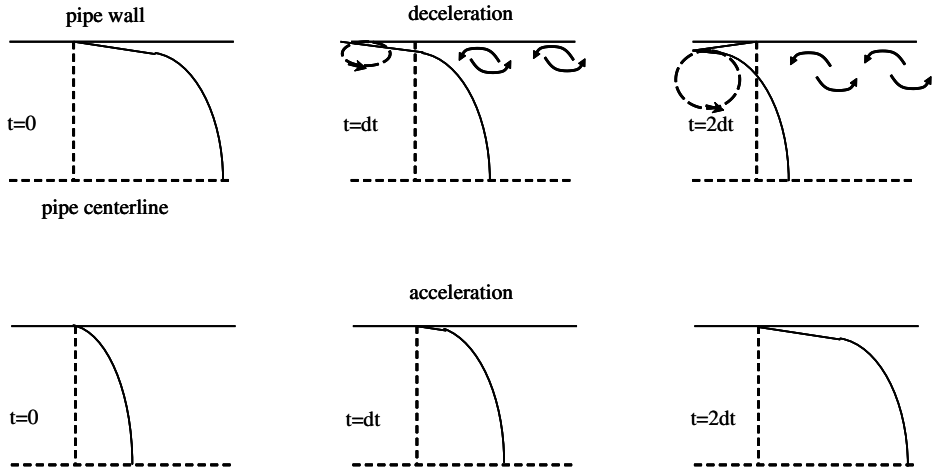


Figure 1 Schematic velocity profiles during deceleration and acceleration

## 4 Novel unsteady friction model

The discussion above motivates a novel model for unsteady shear stresses in turbulent flows with the following features:

- The influence of the initial Reynolds number should fade away after the turbulence diffusion time scale.
- The model should explicitly account for the physical difference between accelerating and decelerating flows.

This section discusses two new concepts, which are exploited in the proposed new unsteady friction model:

- History velocity
- Transient vena contracta

### *4.1 History velocity*

It has been motivated above that many pipeline systems in practice are characterised by a turbulence diffusion-waterhammer time scale ratio of order 1. Consequently the diffusion time scale must be taken into account explicitly. Let us define an artificial, history, velocity that evolves according to the turbulence diffusion time scale towards the instantaneous velocity. If the instantaneous velocity has remained constant for a period of order $D/u_*$, then the history velocity has evolved to the instantaneous velocity. If the instantaneous velocity develops on the time scale of the turbulence diffusion, then the flow develops in a quasi-steady way and no unsteady friction effects are assumed to be absent. The larger the difference between the instantaneous velocity and the history velocity, the more important unsteady friction becomes. The history velocity is initialised to the steady state velocity. The simplest model for this history velocity is a linear differential equation, such that the history velocity develops exponentially towards the instantaneous velocity at a rate proportional to the diffusion time.

$$\frac{dv_h(t)}{dt} = (v(t) - v_h(t))\,\frac{d \cdot u_{*,h}}{D} \tag{13}$$

where $d$ is a calibration parameter for the rate at which the history velocity profile evolves towards the instantaneous velocity. Let us call this parameter, $d$, the decay parameter, because the history velocity decays towards the instantaneous velocity. He's experiments with 2 s ramp up flow excursions (He and Jackson, 2000) show that the turbulence structure has stabilised 1.3 s after the flow excursion. If it is presumed that the 2 s ramp up time corresponds with an instantaneous flow increase after 1 s, then the exponential decay value for the turbulence structure ($d$) equals 1.4 according to He's measurements. The assumption, that a 2 s ramp up is equivalent with an instantaneous flow increase after 1 s, is disputable, but the rational shows that the decay parameter must be of this order of magnitude.

The history velocity equation may be solved using Euler integration. A more robust solution is obtained from direct integration leaving $v(t)$ and $u_*$ constant during one time step $\Delta t$:

$$v_h(t + \Delta t) = v(t) - (v(t) - v_h(t)) \cdot e^{-\frac{d \cdot u_{*,h} \cdot \Delta t}{D}} \tag{14}$$

### *4.2 Transient vena contracta during pressure wave passage*

The concept of the transient vena contracta aims to contribute to the new physically-based unsteady friction model, addressing the physical difference between decelerating and accelerating flows. During a transient deceleration vortices develop in the wall region, while the core velocities are decelerated in an undisturbed way, because the turbulence structure needs time to propagate towards the pipe centreline. The instantaneous velocity profile during a deceleration is assumed to be very similar to a steady velocity profile downstream of an orifice plate (or other concentric obstruction) with such a throat diameter that the steady vortices downstream of the orifice have the same size as the transient vortices in the decelerating flow. The assumption that the transient deceleration vortices have a similar shape as the steady deceleration vortices, leads to the idea to model the transient energy dissipation in analogy with the steady energy dissipation. The transient vena contracta represents the contraction of the flow during a deceleration faster than the turbulent diffusion time. During these rapid decelerations a variable wall annulus can be identified without any net liquid transport. Hence 100% of the flow is transported through the contracted core region. The novel unsteady friction model associates an energy loss to this transient vena contracta. The transient vena contracta and the core region

shrink as the deceleration progresses. The main assumption of this paper is that the transient energy loss is related to the transient vena contracta in a similar way as the steady energy loss caused by the same vena contracta.

The steady head loss associated with a vena contracta of size $\mu$ ($\mu = A_c/A$) is defined by the well known Borda–Carnot equation:

$$\Delta H = \left(1 - \frac{1}{\mu}\right)^2 \frac{v|v|}{2g} \tag{15}$$

where $v$ refers to the average pipe velocity. The vena contracta is defined as the smallest fraction of the cross section that transports the total flow rate.

$$\begin{aligned} \mu &= \left(\frac{r^*}{R}\right)^2 \\ Q &= 2\pi \int_0^{r^*} v(r) \cdot r \cdot dr \end{aligned} \tag{16}$$

where $v(r)$ refers to the local velocity at radius $r$. The transient head loss due to unsteady friction is assumed to be proportional to the Borda–Carnot head loss and furthermore proportional with the length-diameter ratio of a pipe element, such that:

$$\Delta H_{uf} = \phi \cdot K \left(1 - \frac{1}{\mu}\right)^2 \frac{v|v|}{2g} \frac{\Delta x}{D} \quad \text{or} \tag{17}$$

$$\tau_{uf} = \phi \cdot K \left(1 - \frac{1}{\mu}\right)^2 \frac{\rho v|v|}{8} \quad \text{or} \tag{18}$$

$$f_{uf} = \phi \cdot K \left(1 - \frac{1}{\mu}\right)^2 \tag{19}$$

where $\mu$ is the transient vena contracta due to flow deceleration, $\phi$ models the correct sign of unsteady friction and $K$ is a proportionality parameter, a damping coefficient, preferably of universal nature. The remaining problem is to find a model for the transient vena contracta $\mu$. The sign of the unsteady friction factor will be discussed in Section 4.3.

The transient vena contracta is quantified as follows. A certain steady velocity profile is decelerated instantaneously, creating a wall annulus with a net flow equal to zero. Some relation is required between the friction factor (or friction velocity) and the velocity profile. A rough approximation that relates the steady friction factor to a power law velocity profile is:

$$\begin{aligned} n &= \frac{1}{\sqrt{f_h}} = \frac{v_h}{u_{*,h}\sqrt{8}}; \quad u_{*,\mathrm{h}}(t) = v_h(t)\sqrt{\frac{f_h}{8}} \\ v_h(r) &= v_h(0)\left[1 - \left(\frac{r}{R}\right)\right]^{1/n} \\ v_h &= v_h(0)\frac{2n^2}{(n+1)(2n+1)} \end{aligned} \tag{20}$$

Note that the history velocity is used in Eq. (20). A sudden deceleration shifts almost the complete velocity profile backward without any change in the velocity profile, because the turbulence needs time to travel from the pipe wall to the core region. The following equations hold for the average velocity and the instantaneous velocity profile in the core region, after a sudden deceleration:

$$\begin{aligned} v(t) &= v_h + \frac{dv}{dt}\Delta t = v_h + dv \\ v(r,t) &= v_h(r) + dv \end{aligned} \tag{21}$$

The thickness of the wall annulus that is affected by the turbulence diffusion during time step $\Delta t$ is of the order of magnitude $u_{*,h} \cdot \Delta t$. It is important to note that the deceleration is based on the difference between the average instantaneous velocity and the history velocity. Since the net discharge flows through the core region, an expression for the transient vena contracta is found from:

$$\begin{aligned} Q(t) = A \cdot v(t) &= 2\pi \int_0^{r^*(t)} v(r,t) \cdot r \cdot dr \\ &= 2\pi \int_0^{R\sqrt{\mu(t)}} v(r,t) \cdot r \cdot dr \end{aligned} \tag{22}$$

Partial integration and substitution of the power law velocity profile (average $v$ in power law and max $v$) yields the following expression for the dimensionless radius:

$$x = \frac{r^*}{R} = \sqrt{\mu_x(t)} \tag{23}$$

$$v_h\left[\frac{n+1}{n}x + 1\right](1-x)^{\frac{1}{n}} + dv \cdot (x+1) = 0 \tag{24}$$

The vena contracta is arbitrarily bounded at a value 0.25 ($x > 0.0625$), to prevent division by zero if the instantaneous average velocity equals zero and the transient vena contracta would become zero. Equation (24) is formally valid for flow decelerations until the turbulence has propagated into the core region. Practical power law values vary from $n = 5$ to $n = 10$. Solutions of Eq. (24) for different values of the power law coefficient are presented in Fig. 2.

According to Fig. 2, the flow must decelerate 70 to 85% before the transient vena contracta drops to 0.8. If the dimensionless deceleration ($dv/v_h$) is less than 40%, the transient vena contracta remains practically equal to unity and no extra damping will be predicted. It is recalled that this transient vena contracta is based on a shift of the steady velocity profile only. In reality, another physical process occurs simultaneously, which will be discussed and included below.

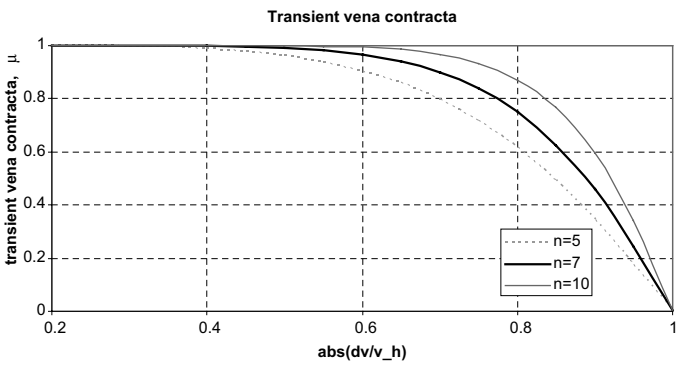


Figure 2 Transient vena contracta as a function of the dimensionless deceleration

### *4.3 Transient vena contracta after passage of a decelerating pressure wave*

The physical process that forces the flow contraction and transient vena contracta to return to the full pipe cross-sectional area, corresponding with $\mu = 1$, is the turbulent viscosity, which propagates from the wall towards the centreline, adjusting the instantaneously shifted velocity profile towards a new steady velocity profile. The shear pulse starts from the wall, due to the shifted velocity profile, and travels towards the pipe centreline, adjusting the local turbulence structure. The rate at which the shear pulse propagates towards the centreline has been measured by He and Jackson (2000) and equals:

$$\frac{R}{T_d} = \frac{D}{2}\frac{u_*\sqrt{2}}{D} = \frac{u_*}{\sqrt{2}} \tag{25}$$

The velocity profile is adjusted by the shear pulse propagation in an unknown way. This model focuses on the situation where the turbulence diffusion time is smaller than the pipe period ($P < 1$). In such a situation the locally distorted velocity profile evolves towards the new velocity profile before the next reflected pressure wave distorts the velocity profile again. It is assumed for simplicity that the same power law coefficient, $n$, applies to both the original steady velocity and the new decelerated velocity; this implies in fact that the flow remains fully turbulent, in accordance to Eq. (20).

Immediately after the deceleration the velocity profile is shifted by $dv$ ($dv = v_1 - v_2$) with an infinitely steep gradient at the pipe wall. Only one local velocity is shifted to the correct new local velocity; this occurs at the pipe radius at which the local velocity equals the pipe average velocity; see Fig. 3. This (dimensionless) radius, $x$, equals 0.75, almost irrespective of the power law coefficient; see table Table 1.

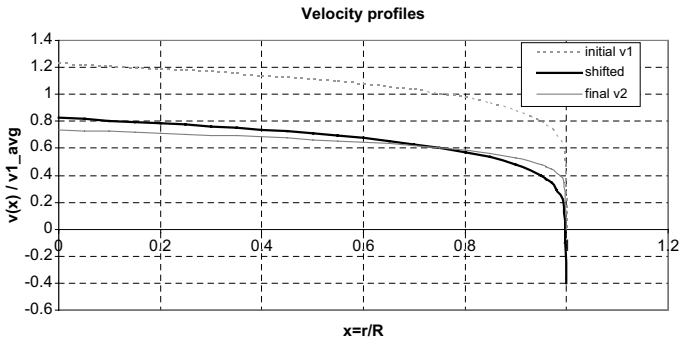


Figure 3 The initial, shifted and final velocity profiles for $n = 7$ and $dv = 0.4 * v_1$

Table 1 Dimensionless radius where the local steady velocity equals the average velocity

| $n$ | $x$ at which $v(x) = \bar{v}$ |
|---|---|
| 5 | 0.750 |
| 7 | 0.757 |
| 10 | 0.763 |

At radii $r > 0.75R$ the local axial velocity must increase, whereas at radii $r < 0.75R$ the local axial velocity must gradually decrease towards the new velocity profile, as illustrated in Fig. 3.

The shear pulse propagates at constant rate from the wall ($x = 1$) towards the centreline ($x = 0$), according to Eq. (25). The shifted velocity profile remains constant until the shear pulse has passed. Furthermore the average velocity must remain constant and equal to $v_2$. Consequently, any adjustment of the shifted local velocity towards the final velocity profile may only occur in the shear pulse zone between the shear pulse front and the pipe wall. The local velocity near the pipe wall must increase immediately after the deceleration and consequently the velocities near the shear pulse front must further decelerate, although the shifted local velocity is smaller than the final local velocity; see Fig. 3. If the calculated TVC, based on the shifted velocity profile, extends into the shear pulse zone, then the real TVC must be larger, because the velocity reduction near the shear pulse front increases the TVC. The further the shear pulse front has propagated towards the centreline, the larger is its effect on the TVC. He's measurements show that the local velocities and turbulence structure have stabilised to their new values some time after the end of the manoeuvre; see the section *History velocity*. The observations above motivate the assumption that the TVC rises exponentially towards the new steady state value (unity) in a way similar as the history velocity. This exponential increase is included in the model as follows:

$$\mu(t + \Delta t) = \min\left\{\mu_x(t + \Delta t);\, 1 - (1 - \mu(t)) \cdot e^{-\frac{d \cdot u_{*,h} \cdot \Delta t}{D}}\right\} \tag{26}$$

The transient vena contracta and history velocity are defined in every calculation node.

### *4.4 The sign of the unsteady friction factor*

The unsteady friction contribution has been discussed as if it was a term representing energy dissipation. However the waterhammer equations include a continuity and momentum equation only. It is necessary to assign the correct sign to the dissipating force in the momentum equation. Since the pipe wall exerts a shear stress on the fluid layer at the pipe wall, the direction of the dissipating force must be based on the (assumed) flow direction close to the wall.

When the flow decelerates, the velocity close to the wall has the opposite sign of the average velocity. Therefore the unsteady friction factor is negative and partially cancels the quasi-steady friction factor. When the flow accelerates, the wall velocity has the same direction as the average velocity and the unsteady friction factor has the same (positive) sign as the quasi-steady friction factor. Since the acceleration or deceleration is based on the difference between the history velocity and instantaneous average velocity, the arguments above result in the following definition of $\phi$.

$$\begin{aligned} &\phi = -1, \quad \textit{if } \{(|v| - |v_h| < 0) \wedge (v \cdot v_h > 0)\} \\ &\phi = +1, \quad \text{otherwise} \end{aligned} \tag{27}$$

## 5 Validation

The above described model has been validated against eight transient scenarios in four different systems. The initial Reynolds numbers are ranging from 1940 to 1,470,000. The four systems are briefly discussed hereafter.

### *5.1 Perugia system*

This test rig for fluid transients, operated by the University of Perugia, department of civil and environmental engineering (Dipartimento di Ingegneria Civile ed Ambientale), has been described extensively in the literature on unsteady friction modelling; see Brunone *et al.* (2000, 2001). Its length is 350 m, internal diameter is 93.5 mm and the wave celerity in the PE pipe is 320 m/s. The transient measurements comprise a fast and a moderate valve closure. The measurements have been extracted from the EU Transdat database on fluid transients Brunone *et al.* (2001). The initial Reynolds numbers of the two scenarios from this test rig are 49,000 and 112,000. The drawback of this system for proper validation is the unknown visco-elastic behaviour of the PE pipe wall.

### *5.2 Adelaide system*

A flexible laboratory apparatus for investigating water hammer and column separation events in pipelines has been designed and constructed at the University of Adelaide, Department of Civil and Environmental Engineering. The apparatus comprises a straight 37.23 m long sloping copper pipe of 22.1 mm internal diameter and 1.63 mm wall thickness connecting two pressurized tanks. Water hammer events in the apparatus are initiated by rapid closure of the ball valve. The system is described in more detail in several papers, including Bergant *et al.* (2001). The benefit, compared to the Perugia system, is the elastic behaviour of the copper pipe wall, but the Reynolds numbers are relatively small: 1940, 3880, and 5700.

### *5.3 CAPWAT system*

This large scale laboratory system, operated by WL|Delft Hydraulics, has been built primarily for testing air pocket detection methods in sewage transmission pipelines. CAPWAT is an acronym for CAPacity losses in wasteWATer transport pipelines. The system length is 645 m (625 m PVC and 20 m steel), inner diameter is 235.4 mm (PVC) and the wave celerity is 317 m/s. The pumped system includes a few large radius bends and has been built in a horizontal plane. The pump has a variable speed drive, which can be ramped up or down within 1 s. The CAPWAT system is equipped with four pressure tranducers after 5 m, 104 m, 224 m, and 520 m. The sample frequency of the pressure tranducers is 100 Hz. The flow meter, which is installed to measure the initial flow rate, is not suitable for transient measurements. The facilities for introducing air pockets were not used during these measurements. The system has been described in detail in Lubbers' paper (2005).

The first transient scenario is a pump ramp down from 1560 rpm to 0 rpm in 1 s with a throttled downstream butterfly valve such that the initial flow rate is approximately 32 l/s. After 30 s the flow rate has dropped stepwise to 3 l/s without any flow reversal. The second transient scenario is a pump ramp up from 740 rpm to 1325 rpm within 0.5 s with a fully open downstream valve. Again the initial flow rate is approximately 32 l/s which rises stepwise to 60 l/s after 30 s.

### *5.4 Bath (NL) sewage system*

This system is a 14.9 km concrete pipeline carrying treated wastewater from Bath (NL) to the Westerschelde. The internal diameter is 1800 mm over the first 2.1 km; the internal diameter of the remaining 12.8 km is 1500 mm. The system includes two pumps (one in operation, one stand-by), hydraulically damped check valves with unknown damping characteristics, a by-pass check valve and no other anti-surge devices. In 1996 and 1997 many steady state measurements and several transient measurements have been carried out by WL|Delft Hydraulics (part of Deltares since 1st January 2008). The transient measurements were conducted to verify whether the observed head losses were caused by gas pockets. The transient measurements showed that the pipeline does not contain any free gas. The flow rate is measured in the pumping station and pressure tranducers were installed after 1.5 km, 3 km, and 12 km. The transient scenario, included in this paper, is a pump trip scenario at an initial flow rate of 1.67 $m^3$/s. A small industrial treatment plant injected 0.07 $m^3$/s after 2.1 km. No information could be retrieved on the dynamic behaviour (pump curve and control settings) of the industrial treatment plant; the assumption has been made that the discharge pressure does remain constant, such that the flow increases as the system pressure drops. The flow meter indicates that the flow rate at the pumping station has dropped to 200 l/s after 180 s.

The transient operations are summarised in Table 2. All manoeuvres occur mainly within the first pipe period and are therefore fast manoeuvres.

## 6 Discussion

As illustrated in Fig. 2 a flow deceleration of 80% is required to get any damping at all. The practical consequence is that the proposed unsteady friction model only predicts any extra damping if flow reversal occurs. This implies that the CAPWAT and Bath scenarios should be reasonably reproduced with a quasi-steady friction model, because flow reversal does not occur in these scenarios. The new unsteady friction model has been included in WANDA, developed by Deltares|Delft Hydraulics.

### *6.1 Perugia system*

The damping coefficient, $K$, and the decay coefficient $k_1$, have been calibrated to match the valve closure in 0.43 s. This has resulted in a damping coefficient $K = 0.05$ and decay coefficient

Table 2 Overview of transient operations

| System | Manoeuvre | Initial flow [l/s] | Reynolds [−] | Wave speed [m/s] | Manoeuvre time [s] | Pipe period [s] | Time scale ratio, $P$ [−] |
|---|---|---|---|---|---|---|---|
| Perugia | Valve closure | 3.6 | 49,000 | 320 | 0.43 | 2.2 | 1.9 |
| Perugia | Valve closure | 8.2 | 112,000 | 320 | 1.66 | 2.2 | 0.9 |
| Adelaide | Valve closure | 0.038 | 1,940 | 1282 | 0.006 | 0.058 | 83.7 |
| Adelaide | Valve closure | 0.077 | 3,880 | 1282 | 0.006 | 0.058 | 38.3 |
| Adelaide | Valve closure | 0.115 | 5,810 | 1282 | 0.006 | 0.058 | 26.7 |
| CAPWAT | Pump ramp down | 31.9 | 173,000 | 317 | 1.0 | 4.1 | 2.4 |
| CAPWAT | Pump ramp up | 32.4 | 175,000 | 317 | 0.5 | 4.1 | 2.4 |
| Bath NL | Pump trip | 1667 | 1470,000 | 1170 | 30* | 25.5 | 2.0 |

*The pump speed has dropped to 10% after 30 s.

$d = 0.8$. The first pipe period, the unsteady friction model (legend: UF), the quasi steady model and the measurement are almost identical. As anticipated the quasi-steady friction model does not predict sufficient damping. The unsteady friction model predicts slightly more damping during the second to the fourth oscillations and slightly less damping during the later oscillations. The overall results is a clearly better reproduction of the damping, although the shape of the pressure trace is not perfectly reproduced, probably due to the fact that the exponential rise of the TVC is too much simplified. The measurement reveals a more and more regular pressure trace after 4 or 5 oscillations, possibly due to axial diffusion and dispersion of momentum, which is not included in the proposed model. Another reason for the observed differences is that the maximum calculated velocity has dropped to 0.1 m/s (Re $<$ 9500) after 25 s, implying that the viscosity may play a more important role. The proposed unsteady friction model does not include any viscosity driven friction effects, that may cause additional damping after 4 oscillations.

The calibrated parameter values have been applied in the other simulations. The valve closure in 1.66 s is fairly well reproduced. It is surprising that the measurement shows already some damping during the first pipe period. It is furthermore surprising that the measurement tends towards a slightly greater wave speed (negative phase shift), which contradicts other observations in literature. Again the unsteady friction model predicts the damping significantly better than the quasi steady model.

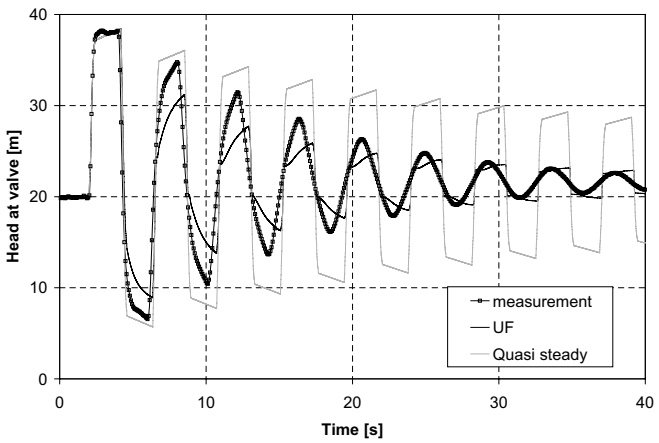


Figure 4 Perugia system 0.43 s closure—Head at valve

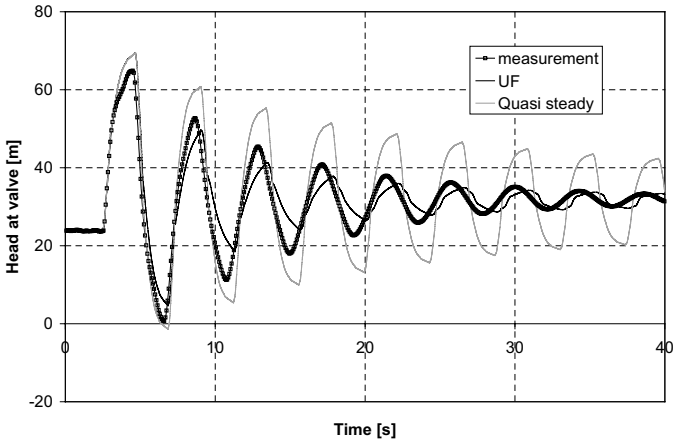


Figure 5 Perugia system 1.66 s closure—Head at valve

### 6.2 *Adelaide*

The same parameter settings ($K = 0.05$; $d = 0.8$) have been applied in the three simulations of the Adelaide experiments in a copper pipe at very low Reynolds numbers. Again, the novel unsteady friction model clearly outperforms the quasi-steady friction model. As the velocity increases, the damping of the simulation model tends towards the measured damping; see Figs 6 to 11. The simulated heads in the midpoints show sharp transitions on each wave passage, which confirms that the implementation of the MOC based numerical scheme causes no numerical dispersion. The midpoint measurements show limited dispersion, because the sharp transitions during the first and second wave period become more gradual during the following wave periods.

### 6.3 *CAPWAT*

The measurement of the 1 s pump ramp down is extremely well reproduced by both the quasi-steady and the unsteady friction model. The measurement of the 0.5 s ramp up only shows some discrepancy during the second oscillation, but this has diminished after 3 oscillations. The CAPWAT measurements confirm that unsteady friction is not a dominant damping mechanism if flow reversal does not occur in high Reynolds number flows.

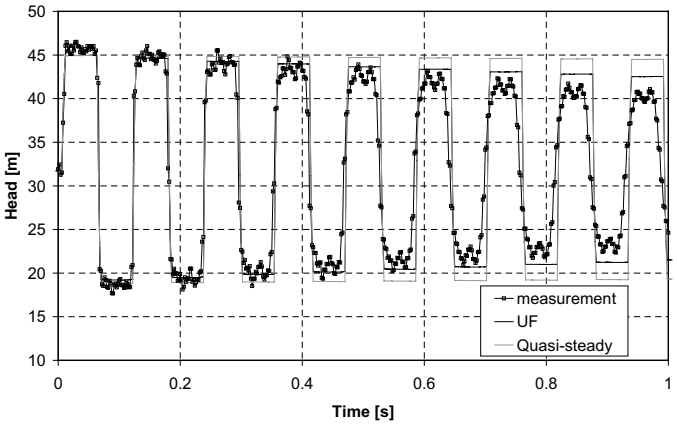


Figure 6 Adelaide system valve closure at 0.1 m/s—Head at valve

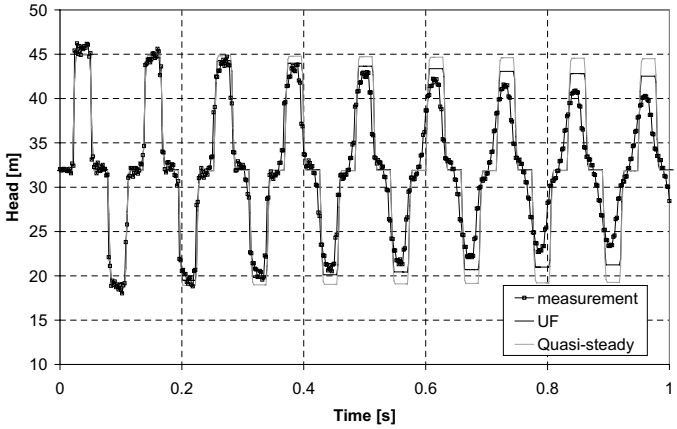


Figure 7 Adelaide system valve closure at 0.1 m/s—Head at valve

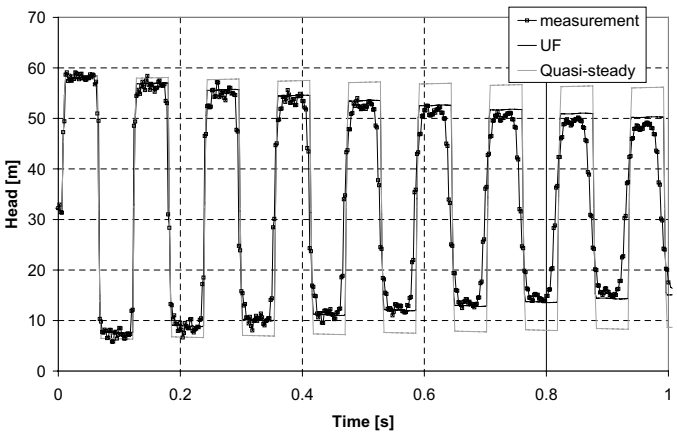


Figure 8 Adelaide system valve closure at 0.2 m/s—Head at valve

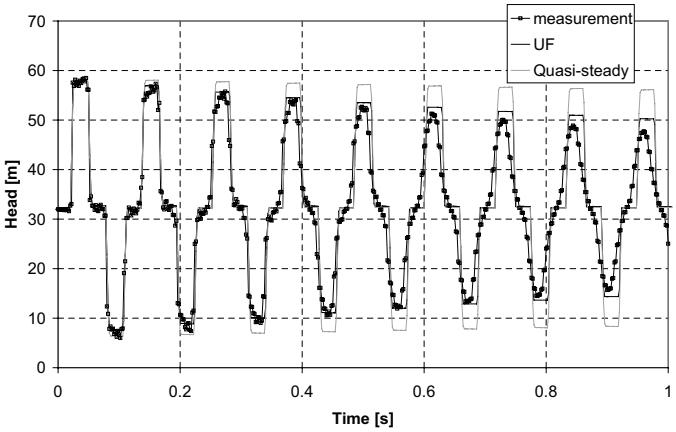


Figure 9 Adelaide system valve closure at 0.2 m/s—Midpoint head

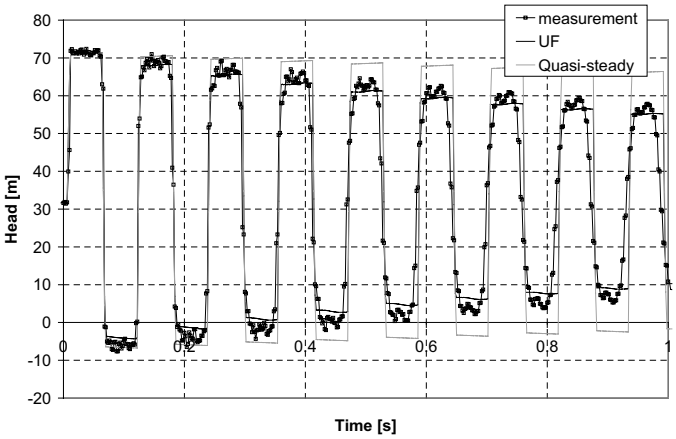


Figure 10 Adelaide system valve closure at 0.3 m/s—Head at valve

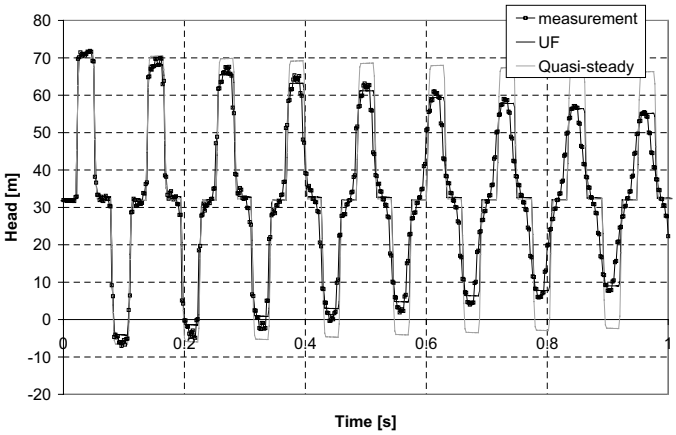


Figure 11 Adelaide system valve closure at 0.3 m/s—Midpoint head

### *6.4 Bath (NL)*

Similar to the CAPWAT scenarios, the unsteady friction model produces identical results as the quasi steady model, because flow reversal does not occur. The difference between the measurement and the quasi-steady model is marginal, given the fact that many parameters are not known accurately and have been assessed based on expert judgement.

These measurements indicate that unsteady friction is less dominant in high Reynolds number flows, if the flow does not reverse during the transient event.

## 7 Conclusions and recommendations

Unsteady friction is dominant during fluid transients with flow reversal, such as valve closure scenarios. Quasi-steady friction models show a reasonable accuracy of the pressure damping during high Reynolds number (>100,000) fluid transient without flow reversal, such as pump trip or start-up scenarios.

The statement that a phase-shift develops due to unsteady friction is not confirmed by any of these comparisons.

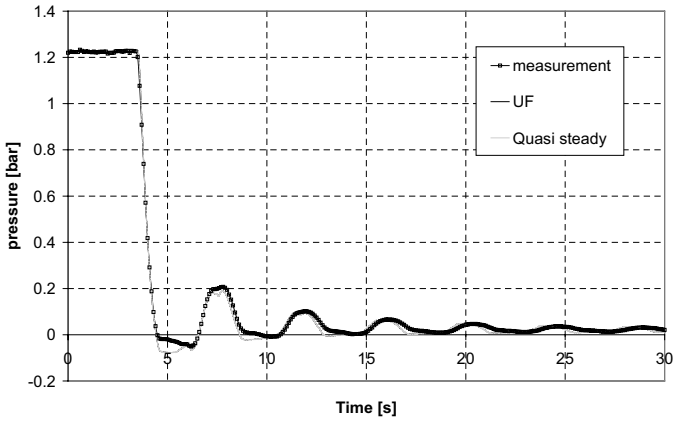


Figure 12 CAPWAT system 1 s ramp down—Pressure at 223.6 m

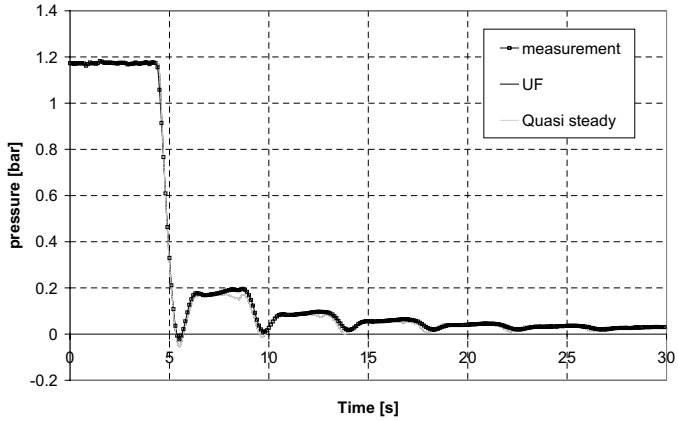


Figure 13 CAPWAT system 1 s ramp down—Pressure at 519.7 m

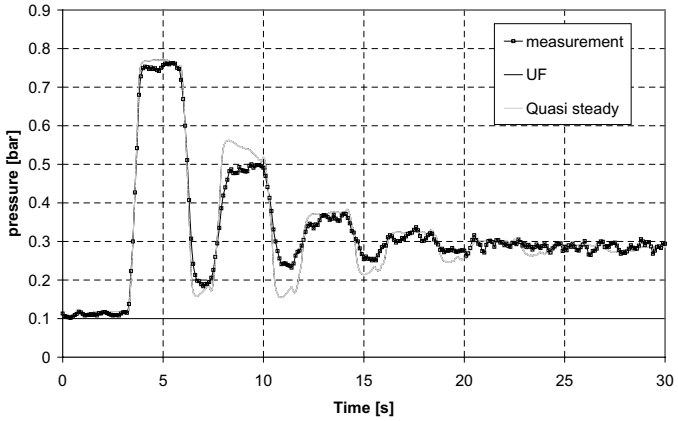


Figure 14 CAPWAT system 0.5 s ramp up—Pressure at 223.6 m

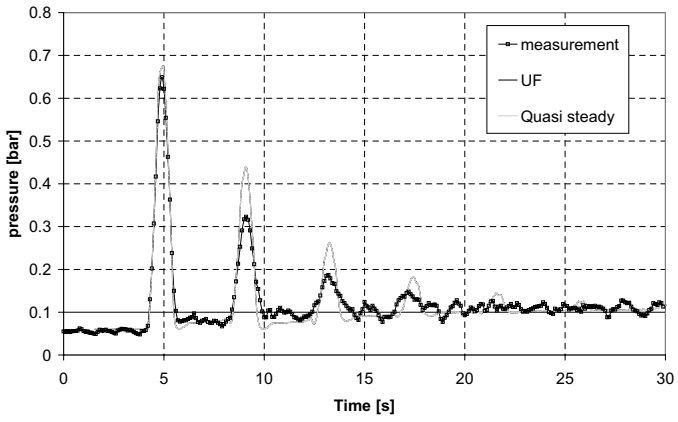


Figure 15 CAPWAT system 0.5 s ramp up—Pressure at 519.7 m

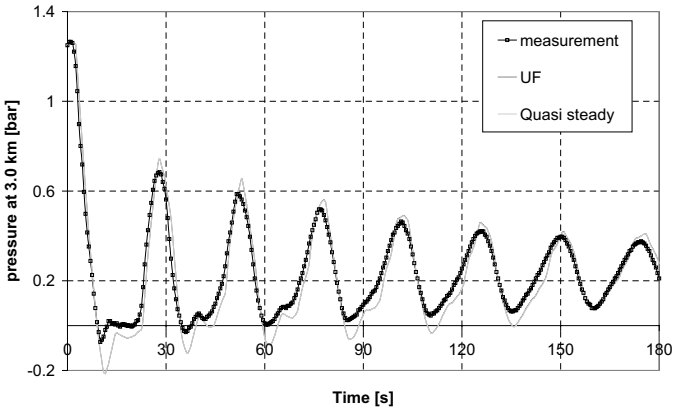


Figure 16 Bath (NL) system pump trip—Pressure at 3 km

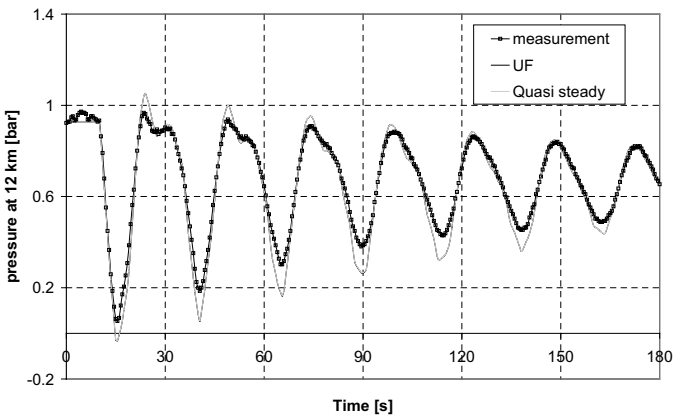


Figure 17 Bath (NL) system pump trip—Pressure at 12 km

This paper has proposed and validated a novel unsteady friction model that is entirely based on turbulent flow considerations. The proposed model exploits two new concepts:

- The *history velocity*, which is the velocity that evolves towards the instantaneous velocity at the turbulent diffusion time scale. The turbulent diffusion time scale is generally longer than the time scale of a transient operation (e.g., pump trip or valve closure), which is a necessary condition for unsteady friction as an additional term to quasi-steady friction.
- The *transient vena contracta* represents the contraction of the flow during a deceleration faster than the turbulent diffusion time. During these rapid decelerations a variable wall annulus can be identified without any net liquid transport. Hence 100% of the flow is transported through the contracted core region. The novel unsteady friction model associates an energy loss to this transient vena contracta.

The main features of the proposed unsteady friction model, as opposed to existing unsteady friction models, include the dissipation of the influence of the initial steady state and the distinction

between decelerating and accelerating flow. The new unsteady friction model reproduces the valve closure scenarios in the Perugia and Adelaide laboratory systems clearly better than the quasi-steady friction model. The measurements show some dispersion which is not incorporated in the model. The numerical model contains no numerical dispersion, as expected from a MOC-based model.

Further research is recommended to include the measured dispersion. The proposed unsteady friction model is based on a set of rough assumptions that need to be further investigated and refined to give the model a more solid theoretical background. Particularly the concept of the transient vena contracta requires further research. Nevertheless the results show a significant improvement over the quasi-steady friction model.

## Notation

$A$ = Cross-sectional area ($m^2$)
$c$ = Wave propagation speed (m/s)
$C^*$ = Non-dimensional shear decay coefficient
$d$ = Unsteady friction decay parameter
$D$ = Pipe diameter (m)
$f$ = (Darcy-Weisbach) friction factor
$g$ = Gravity acceleration ($m/s^2$)
$H$ = Head (m)
$k$ = Unsteady friction coefficient
$K$ = Unsteady friction proportionality parameter
$L$ = Pipe length (m)
$M$ = Mach number, $v/c$
$n$ = Power law coefficient
$P$ = Turbulence diffusion—waterhammer time scale ratio
$Q$ = Flow rate ($M^3/s$)
$r$ = Radius ($0 \leq r \leq R$) (m)
$R$ = Pipe radius (m)
Re = Reynolds number
$t$ = Time (s)
$T_d$ = Delay of turbulence diffusion at the pipe centreline (s)
$u_*$ = Friction velocity (m/s)
$v$ = Velocity (m/s)
$v_s$ = Sensitivity velocity (m/s)
$W(\theta)$ = Weighting function
$x$ = Dimensionless pipe radius
$\Delta x$ = Discretisation element length (m)
$\alpha$ = Friction decay coefficient
$\phi$ = Sign of unsteady friction factor
$\kappa$ = Parameter to approximate the shear decay coefficient
$\mu$ = Transient vena contracta (TVC)
$\nu$ = Kinematic viscosity ($m^2/s$)
$\rho$ = Fluid density ($kg/m^3$)
$\tau$ = Shear stress (Pa)
$\psi$ = Non-dimensional historical time

*Subscripts*

$d$ = Turbulent diffusion
$h$ = History
$lam$ = Laminar
$lim$ = Limiting (in time)
$qs$ = Quasi-steady
$s$ = Steady state preceding the transient event
$tot$ = Total
$uf$ = Unsteady friction

## References


Bergant, A., Simpson, A.R., Vitkovsky, J. (2001). Developments in unsteady pipe flow friction modelling. *J. Hydraul. Res.* 39(3), 249–257.

Brunone, B., Golia, U.M., Greco, M. (1991). Some remarks on the momentum equation for fast transients. *Proceeding of Internation Conference on Hydraulic Transients with Water Column Separation*, IAHR, Valencia, Spain, 201–209.

Brunone, B., Karney, B.W., Mercarelli, M., Ferrante, M. (2000). Velocity profiles and unsteady pipe friction in transient flow. *J. Water Resources Planning and Management, ASCE* 126(4), 236–244.

Brunone, B. *et al.* (2001). Transient pressures in pressurised conduits for municipal water and sewage water transport. WP3 Collect and analyse transient data, EC project SMT4-CT97-2188, report number 8664–47.

Carsten, M.R., Roller, J.E. (1955). Boundary shear stress in unsteady turbulent pipe flow. *J. Hydraul. Div., ASCE* 85(HY2), 67–81.

Daily, J.W., Hankey, W.L., Olive, R.W., Jordaan, J.M. (1956). Resistance coefficients for accelerated and decelerated flows through smooth tubes and orifices. *Trans. ASME* 78, 1071–1077.

Ghidaoui, M.S., Mansour, S.G.S., Zhao, M. (2002). Applicability of quasi-steady and axisymmetric turbulence models in water hammer. *J. Hydraul. Engng.* 128(10), 917–924.

Ghidaoui, M.S., Zhao, M., McInnis, D.A., Axworthy, D.H. (2005). A review of water hammer theory and practice. *Applied Mechanics Reviews*, 58, 49–76.

He, S., Jackson, J.D. (2000). A study of turbulence under conditions of transient flow in a pipe. *J. Fluid Mech.* 408, 1–38.

Lubbers, C.L. (2005). On detecting gas pockets in pressurised wastewater mains. *Proceedings of the 10th International Conference on Urban Drainage*, Copenhagen, Denmark, August 21–26.

Pezzinga, G. (2000). Evaluation of unsteady flow resistances by quasi-2D or 1D models. *J. Hydraul. Engng.* 126(10), 778–785.

Shuy, E.B. (1996). Wall shear stress in accelerating and decelerating turbulent pipe flows. *J. Hydraul. Res.* 34, 173–183.

Shuy, E.B. (1995). Approximate wall shear equation for unsteady laminar pipe flows. *J. Hydraul. Res.* 33, 457–469.

Vardy, A.E., Brown, J.M.B. (1995). Transient turbulent smooth pipe friction. *J. Hydraul. Res.* 33, 435–456.

Vardy, A.E. *et al.* (1996). On turbulent, unsteady, smooth pipe friction. *Proc. 7th Int. Conf. on Pressure Surge and Fluid Transients*, 289–311.

Vardy, A.E., Brown, J.M.B. (2003). Transient turbulent friction in smooth pipe flows. *J. Sound and Vibration* 259(5), 1011–1036.

Vardy, A.E., Brown, J.M.B. (2004). Transient turbulent friction in fully rough pipe flows. *J. Sound and Vibration* 270(1–2), 233–257.

Vardy, A.E., Brown, J.M.B. (2007). Approximation of turbulent wall shear stresses in highly transient pipe flows. *J. Hydraul. Engng.* 133(11), 1219–1228.

Vardy, A.E., Hwang, K.L., Brown, J.M.B. (1993). A weighting function model of transient turbulent pipe friction. *J. Hydraul. Res.* 31, 533–548.

Vítkovský, J.P., Bergant, A., Simpson, A.R., Lambert, M.F. (2006). Systematic evaluation of one-dimensional unsteady friction models in simple pipelines. *J. Hydraul. Engng.* 132(7), 696–708.

Zielke, W. (1968). Frequency dependent friction in transient pipe flow. *ASME J. Basic Engng.* 90(1), 109–115.